the ORNL Director's R&D Fund. This research was also supported in part by an appointment of J.M.B. to the Postgraduate Research Training Program under Contract DE-AC05-76OR00033 between the U.S. Department of Energy and Martin Marietta Energy Systems, Inc., and of V.A.N. to the ORAU 1989 Summer Faculty Research. In addition, research participation of D.L.S. was supported by Subcontract 95XSD430 through Martin Marietta Energy Systems, Inc.

Flow Dependence and Sensitivity of the Refractive Index Gradient Measurement with the Z-Configuration Flow Cell at Low Reynolds Number

Darrell O. Hancock, Curtiss N. Renn, and Robert E. Synovec*

Department of Chemistry, BG-10, Center for Process Analytical Chemistry, University of Washington, Seattle, Washington 98195

A simple model based upon Poiseuille flow is reported that allows the prediction of the sensitivity in the refractive index gradient (RIG) measurement with the Z-configuration flow cell. The RIG measurement is shown to depend upon carefully probing the radial-concentration gradient (orthogonal to the direction of flow) of an analyte. A fiber optic graded refractive index (GRIN) lens combination provided a narrow collimated beam that facilitated accurate probing of the RIG and far-field observation of the beam deflection, for subsequent comparison to the position-sensitive detector output. The flow rate range investigated was at a low Reynolds number, Re $\leq$ 10 in the cylindrical flow cell bore. Both the predicted and experimentally measured RIG data are directly proportional to linear flow velocity and inversely proportional to both the axial length variance of the analyte concentration and the analyte translational diffusion coefficient. The linear flow velocity and axial length variance dependence on RIG sensitivity were examined, and the model was found to closely predict the experimentally observed RIG sensitivity. Band-broadening contributions in the RIG detector are critically accounted for in the calculations. Measuring the radial concentration gradient was found to be over 2 orders of magnitude more sensitive than measuring the axial concentration gradient of a typical analyte peak for microbore liquid chromatography conditions.

INTRODUCTION

The fundamental work of Taylor (*1*) described the dispersion of an analyte concentration profile subjected to flow through a cylindrical tube. Both axial (along the flow) and radial (orthogonal to the flow) diffusion mechanisms were required to fully describe dispersion. The effort in recent years to further understand and apply this fundamental work in flow injection analysis (FIA) and high-performance liquid chromatography (HPLC) has been geared toward determining the axial concentration profile, where the eye of the detector is pointed orthogonal to the flow (*2–10*). The detailed theoretical simulation of the influence of the laminar flow on the concentration profile leads to a bolus-shaped concentration distribution, rich in information for both axial and radial diffusion (*3*). Measurements of dispersion were based upon the axial concentration distribution (*2*). Tijssen found that helically coiled tubes led to secondary flow patterns which had a profound effect on the axial concentration distribution (*5*). The secondary flow leads to better mixing, as was exploited by Van Den Berg and co-workers in optimizing postcolumn reactor systems for HPLC (*6*). The complexity of the axially measured concentration profile was examined by Golay and Atwood (*7, 8*).

The radial concentration gradient is seldom measured directly, at least not intentionally. This was pointed out by McGuffin and co-workers (*11*), who examined in detail the performance of the Z-configuration flow cell, where the radial concentration gradient produced a dynamic lens. The dynamic lens occurred due to the introduction of a specified concentration profile producing an axially, and thus radially, changing refractive index gradient (RIG), leading to an apparent absorbance change when probed with a light source that overfilled the flow cell aperture. In absorbance detection, when either the flow cell or detector photoactive surface is the limiting aperture, the dynamic lens effect clearly leads to baseline aberrations. As a refractive index (RI) detector, the limiting aperture condition does not lead to useful sensitivity for FIA or HPLC but rather is just a detection problem. This RI problem in absorbance detection has been solved to a great extent by Renn and Synovec with a single fiber optic approach employing a simultaneous two-wavelength absorbance difference measurement (*12*). The two-wavelength approach employed position-sensitive detection (*13, 14*) following wavelength dispersion. In order to achieve adequate RI-based sensitivity with the dynamic lens phenomenon, one must not overfill the flow cell aperture but rather probe the radial concentration gradient with either a narrow, collimated light source or a focused light source. The magnitude of the dynamic lens due to the radial concentration gradient can be measured by two methods, both beginning with probe beam deflection. First, the deflected probe beam can be measured by an interferometric transduction mechanism at a simple photodiode detector. This was the basis of the RIG detector that was reported by Hancock and Synovec (*15, 16*), although recognition of the radial concentration gradient was not made in this initial work. Second, the deflected probe beam can be measured more directly by using a position-sensitive detector (PSD) that provides absolute angular deflection data (*17*). Thus, the principle of operation for the RIG detector will seem quite different depending upon whether an interferometric transduction mechanism (*15, 16*) or a direct beam position detection mechanism (*17*) is used. The direct mea-

0003-2700/90/0362-2441$02.50/0

surement method using a PSD is now preferred, since the data are more reliable and useful. Furthermore, in our application papers (*15–17*) the relationship of the probe beam to the flow cell may be misleading. The work presented in this paper will aim to clarify any ambiguity in our previous reports. There was difficulty in quantitatively comparing the results of Hancock and Synovec (*17*) to the results of Pawliszyn, who pioneered the development of the sensitive RIG detector for FIA and HPLC (*18, 19*). It was the difficulty in making a quantitative comparison between available theory and experimental evidence that suggested a more thorough understanding of the hydrodynamic behavior in the Z-configuration flow cell would be useful. In Pawliszyn's measurements the axial concentration gradient was measured directly. With the Z-configuration flow cell, at suitably low Reynolds number, a Poiseuille flow (*20, 21*) appears to exist that produces a sharp radial concentration gradient in the presence of an axial concentration gradient. When measuring the radial concentration gradient directly (*15–17*), one is actually measuring the axial concentration gradient indirectly, since the existence of the radial concentration gradient requires an axial concentration gradient (*1*). The reliability of the radial concentration gradient measurement with the Z-configuration flow cell will be addressed in this report.

We report a simple model, previously unreported, based upon the work of Taylor (*1*), McGuffin (*11*), and Pawliszyn (*18*), as well as our previous work (*15–17*) that describes the sensitive RIG measurement in the Z-configuration flow cell based upon the existence of the radial concentration gradient. The model resorts to a Gaussian concentration profile for simplicity, due to the complexity of the band-broadening mechanisms in FIA experiments (*2–8*) when the analyte diffusion coefficients are small and span a large range, as in polymer analysis with our molecular weight sensor (*16*). The model does not take into account dramatic changes in flow pattern, since it is based upon Poiseuille flow in the flow cell. The flow rate and diffusion coefficient dependencies of the detection mechanism will be examined for low Reynolds number, Re, with Re $\leq$ 10 in the flow cell under the hydrodynamic conditions employed. The model should also be qualitatively correct for higher Re, as long as the flow is not turbulent. An objective of this work is to experimentally examine the credibility of the detection model. It will be shown that the sensitivity of the RIG measurement at low Reynolds number depends upon the probe beam radial position in the flow cell, parallel and offset relative to the flow cell axis, consistent with the proposed model. An optimum probe position was discovered. A fiber optic–graded refractive index (GRIN) lens combination provides a narrow, collimated beam for this study. The narrow, collimated beam also facilitates far-field observation of the RIG deflection of the probe beam that was iteratively photographed for the injection of a test analyte. The data provide formidable evidence of the magnitude of the RIG response for this detector. The model is shown to accurately predict the relative sensitivity of the RIG signal as a function of the linear flow velocity and band-broadening contributions for a test analyte that was chromatographically retained. The band-broadening contributions due to the RIG detector were carefully taken into account. For conditions where the chromatographic band broadening dominates over the band broadening due to the RIG detector flow cell, the model should be accurate in predicting the absolute angular RIG signal. A calculation of this sort is presented. Finally, a comparison is made between probing the radial concentration gradient and the axial concentration gradient (*18, 19*), and a discussion is given of the utility of the RIG detector for microbore liquid chromatography.

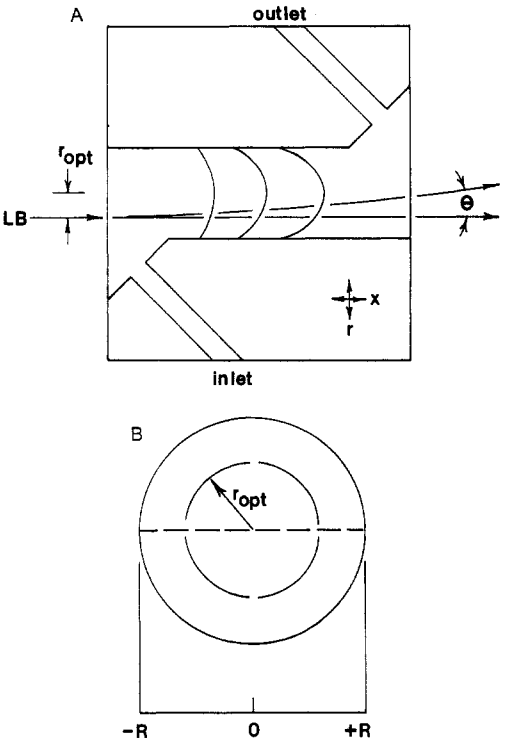

Figure 1. (A) Side view of the Z-configuration flow cell with Poiseuille flow profile inferred: LB, laser beam; r_{opt}, optimum probe beam radial position relative to center optical axis (x axis); θ, deflected probe beam angle. (B) End view of flow cell bore indicating r_{opt} and the horizontal axis examined (dashed line) from $-R$ to $+R$.

THEORY

Poiseuille flow through a cylindrical bore Z-configuration flow cell leads to a parabolic flow profile where the linear flow velocity $u(r)$ is given by (*22*)

$$u(r) = \frac{1}{4\mu}\left(\frac{dp}{dx}\right)(R^2 - r^2) \tag{1}$$

with μ the dynamic viscosity of the solution, dp/dx the axial pressure gradient in the flow cell (*21*), R the radius of the cell, and r the radial position from the center of the flow cell bore. The flow profile as described by eq 1 is depicted in Figure 1A. Taylor (*1*) demonstrated that Poiseuille flow leads to a radial concentration profile $C(r)$ described by

$$C(r) = C(o) + \frac{R^2 u}{4D_m}\left(\frac{r^2}{R^2} - \frac{r^4}{2R^4}\right)\frac{dC(o)}{dx} \tag{2}$$

where u is the average linear flow velocity, D_m is the translational diffusion coefficient of the species of interest, $C(o)$ is the concentration at the center of the flow cell, and $dC(o)/dx$ is the axial concentration gradient existing along the flow cell center axis (x axis in Figure 1). The utility of eq 2 depends upon the relative magnitude of the radial dispersion-induced length variance $\sigma_{x,r}^2$ and the axial dispersion-induced length variance $\sigma_{x,a}^2$ given by (*23*)

$$\sigma_{x,r}^2 = R^2 Lu/24D_m \tag{3}$$

and

$$\sigma_{x,a}^2 = 2D_m L/u \tag{4}$$

where L is the length of a cylindrical tube (either the tubing leading to the flow cell or the flow cell length). Equation 2 is valid when $\sigma_{x,r}^2 \gg \sigma_{x,a}^2$ (*1*), as is typically the case for most liquid-phase experimental procedures of a practical nature.

The optical measurement of the RIG effect requires the existence of a concentration gradient that is orthogonal to a probe beam. With the Z-configuration flow cell, the concen-

tration gradient that is orthogonal to a probe beam is the radial concentration gradient $dC(r)/dr$ that follows from eq 2:

$$\frac{dC(r)}{dr} = \frac{dC(o)}{dx}\left(\frac{ur}{2D_m} - \frac{ur^3}{2R^2D_m}\right) \quad (5)$$

An optimum position to probe $dC(r)/dr$ exists and is found by taking the second derivative of eq 2 and setting $d^2C(r)/dr^2$ equal to 0. Experimental evidence will indicate a fair amount of validity in eq 5 describing the conditions in the flow cell at low Re. The probe beam must be sufficiently smaller than the flow cell bore diameter so the flow cell does not act as an aperture, thus reducing the sensitivity of the subsequent measurement.

The optimum probe beam position occurs at r equal to $R/\sqrt{3}$, or roughly half the distance from the center of the flow cell to the wall of the flow cell. This position is labeled as r_{opt} in Figure 1. Note that eq 5 suggests that probing directly down the flow cell center axis should not produce a RIG response. Although this seems inconsistent with our previous work (Figure 2 in ref 15), it was not clear in initial reports that radial position was important. Careful examination has proven otherwise, and the radial dependence of the RIG sensitivity was critically examined in this work. With a straight-flow geometry, the axial concentration gradient $dC(o)/dx$ was previously measured by Pawliszyn, in the elegant work that has led to the development of RIG detection in HPLC and FIA (*18*, *19*). With the Z-configuration flow, the RIG measurement also depends upon $dC(o)/dx$ as given in eq 5, but the inherent sensitivity of the RIG measurement is not identical for the straight flow geometry (measuring $dC(o)/dx$ directly) and the Z-configuration flow geometry (measuring $dC(o)/dx$ indirectly), since $dC(r)/dr$ is directly measured. The relative sensitivity of the two approaches is given by

$$\frac{dC(r)/dr}{dC(o)/dx} = \frac{1}{2}\left(\frac{1}{\sqrt{3}} - \left(\frac{1}{\sqrt{3}}\right)^3\right)\frac{uR}{D_m} \quad (6)$$

where the $dC(r)/dr$ measurement is made at the optimum r equal to $R/\sqrt{3}$. If the RIG of a Gaussian analyte peak is measured, the axial concentration gradient at $\pm\sigma_x$ from the peak maximum provides the maximum probe beam deflection, where σ_x is the length standard deviation of the detected Gaussian concentration profile in the flow cell (*18*). The solution for the maximum deflection due to $dC(o)/dx$ relative to the baseline is given by

$$\frac{dC(o)}{dx} = \pm\frac{V_iC_ie^{-1/2}}{\sigma_x^2A(2\pi)^{1/2}} \quad (7)$$

where V_i is the volume injected, C_i is the volume fraction of analyte, and A is the cross sectional area of the flow cell equal to πR^2. Combining eqs 6 and 7, the optimally measured radial concentration gradient is then given by

$$\frac{dC(r)}{dr} = \pm 0.0146\left(\frac{V_iC_iu}{\sigma_x^2D_mR}\right) \quad (8)$$

where 0.0146 incorporates all the constants from eqs 6 and 7. The direction of the RIG signal relative to baseline should change sign upon probing along opposite sides of the center axis and go to zero at r equal to 0 (eq 5). It is implied in eq 8 that σ_x^2 is the sum of all band-broadening contributions. In HPLC, σ_x^2 is the sum of the chromatographic broadening and extracolumn broadening such as the broadening due to the flow cell described by eq 3. For HPLC, σ_x^2 is approximately given by (*24*)

$$\sigma_x^2 = \left(\frac{\sigma_v}{\pi R^2}\right)^2 + \frac{R^2Lu}{24D_m} \quad (9)$$

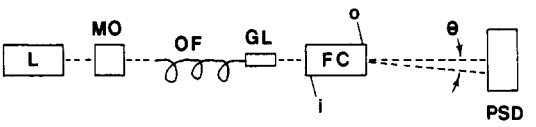

Figure 2. Experimental apparatus: L, HeNe laser; MO, microscope objective; OF, optical fiber; GL, GRIN lens; FC, flow cell with inlet (i) and outlet (o); PSD, position-sensitive detector; θ, angle of the deflected probe beam (shown as a dashed line for clarity, although the light source was not modulated).

where σ_v is the volume standard deviation of the chromatographic peak prior to detection and R is the flow cell radius. In eq 9 it is assumed that the injection and connecting tubing variances can be neglected or are part of σ_v for the purpose of this work. The radial concentration gradient is probed the entire length of the Z-configuration flow cell. The angular deflection, θ, in the RIG measurement for the Z-configuration flow cell is given by (*18*, *19*)

$$\theta = \frac{L}{n_o}\frac{dC(r)}{dr}\frac{dn}{dC} \quad (10)$$

where n_o is the nominal RI of the solvent and dn/dC is the incremental change in RI for a change in analyte concentration in a given solvent. It is assumed that $dC(o)/dx$, and thus $dC(r)/dr$, are constant at any given instant in the flow cell. This assumption will be reasonable when the flow cell does not introduce significant band broadening relative to the chromatographic broadening, as described by eq 9. Thus, eqs 8–10 may be combined to provide a direct means of comparing the experimentally measured angular deflection, θ_{expt}, to the predicted angular deflection, θ_{pred}:

$$\theta_{pred} = \pm 0.0146\left(\frac{V_iC_iu}{\sigma_x^2D_mR}\right)\frac{L}{n_o}\frac{dn}{dC} \quad (11)$$

The utility and limitations of eq 11 will be examined at low Reynolds number. Specifically, the dependence of θ_{pred} on u/σ_x^2 will be compared to θ_{expt} data.

EXPERIMENTAL SECTION

The apparatus applied in this work is similar to that of our previous reports (*15*–*17*) and is shown in Figure 2 with a few important modifications. The 633 nm, 5 mW CW output from a HeNe laser (Uniphase, 1305 P, Sunnyvale, CA) was focused by a 20X microscope objective (Newport Corp., M-20X, Fountain Valley, CA) onto an optical fiber (6 μm core, 125 μm clad, 175 μm jacket) that was designed for single-mode operation at 633 nm (Fujikura, Ltd., SM 6/125 Al coated, Tokyo, Japan). A collimated probe beam was produced by interfacing the optical fiber output to a graded refractive index (GRIN) lens that was quarter pitch at 633 nm (NSG America Inc., Somerset, NJ). (A quarter pitch GRIN lens is designed to provide a collimated beam output from a diverging beam input.) Careful measurement of the beam intensity profile indicated that the probe beam full angle divergence was 3.5 mrad, with an initial diameter of 110 μm, defined as 95% of the beam intensity, at the GRIN lens output face. The narrow, collimated probe beam passed through a Z-configuration flow cell (made in-house) mounted on a high-precision x-y-z translational stage (Newport Corp., 460-XYZ, Fountain Valley, CA) with a 2-cm distance separating the flow cell and the GRIN lens. Two different flow cells were constructed and evaluated. Both were constructed out of aluminum and had a 1.0-cm length (straight bore) with $^1/_{16}$ in. o.d. × 0.007 in. i.d. tubing connected at a 45° angle, as shown in Figure 1. The probe beam is shown at the optimum radial position in Figure 1A for clarity. Note that Figure 1A is a more detailed representation of the experimental conditions than Figure 2 of ref 15, where the probe beam was arbitrarily centered in the flow cell. In our studies the probe beam was examined along the horizontal line in Figure 1B in order to minimize potential distortion to the signal due to the flow at the inlet and outlet, since the inlet was at the bottom and the outlet was at the top of the flow cell, as shown in Figure

1A, i.e. in the vertical plane. The edges within the flow cells were carefully rounded and all evident surface burrs carefully removed and smoothed. Microscope coverslip slides were glued to the flow cell ends to serve as windows. One flow cell had a 1.0 mm i.d. bore (6.3-μL volume), while the other had a 0.8 mm i.d. bore (5.0-μL volume). The probe beam was at an average diameter of 200 μm at the flow cell, so we could readily examine the radial dependence of the proposed detection mechanism given the precision of the translational stage (± 5 μm). The larger 1.0 mm i.d. bore flow cell was used for this purpose, while the smaller 0.8 mm i.d. flow cell was used for the chromatographic detection studies of the flow velocity and band-broadening dependence. After the collimated probe beam passed through the flow cell, it was incident upon a position-sensitive detector (PSD) (Hamamatsu, S1352, Hamamatsu, Japan) with dimensions of 33 mm × 2.5 mm. This PSD was used because it was readily available in our laboratory and we have much experience with this variety (*12–14, 17*). The PSD sensitivity is along the long axis, which was parallel to the horizontal axis shown in Figure 1B.

For the studies of the radial dependence of the probe beam on the detection mechanism sensitivity, a short 100-cm length of 0.007 in. i.d. tubing coiled around a $^1/_2$ in. diameter aluminum rod was used to introduce test analytes to the flow cell from a 1-μL loop at an injection valve (Rheodyne, 7520, Cotati, CA). A syringe pump (ISCO, μLC-500, Lincoln, NE) was used to deliver the deionized water solvent. Test analytes were dextrose (J. T. Baker Co., reagent grade, Phillipsburg, NJ) and 2-propanol (J. T. Baker, reagent grade, Phillipsburg, NJ) in deionized water.

For the studies of the detection mechanism dependence on linear flow velocity, the reversed phase chromatographic retention of toluene (J. T. Baker Co., HPLC grade, Phillipsburg, NJ) with an eluent of 50% acetonitrile to 50% water (by volume) provided the necessary data. A 60 mm × 2 mm column, with 300-Å pore, 5-μm particles with a C8 stationary phase was used (Alltech, Macrosphere, Deerfield, IL). A flow rate range of 75–250 μL/min was examined with all runs done in duplicate. Dilute toluene standard solutions were prepared in 100% acetonitrile and injected with a 4-μL loop at an injection valve (Rheodyne, 7125, Cotati, CA). The toluene chromatograms were recorded by using both a commercially available absorbance detector (ISCO, Model V[4], Lincoln, NE) at 254 nm with a 1-μL flow cell volume and the RIG detector with the 800 μm i.d. flow cell (5.0 μL). The retention volume of the toluene peak was constant throughout at 299 μL (s = 3.7 μL) with a capacity factor of 1.1. The width at the base of the toluene peak was a measure of $4\sigma_v$ for each detector at a given flow rate, where σ_v is the volume standard deviation of a chromatographic peak. Standard laboratory data acquisition techniques were employed. A syringe pump (ISCO, LC-2600, Lincoln, NE) was used to deliver the mobile phase for the chromatography experiment.

RESULTS AND DISCUSSION

According to eq 5, the sensitivity of the RIG measurement with the Z-configuration flow cell should depend upon the radial position of the probe beam. This dependence was examined by first centering, top-to-bottom in the flow cell, the 200 μm diameter collimated probe beam using the 1.0 mm diameter bore flow cell and then injecting 500 ng of dextrose (in water) at 50 μL/min water flow rate at several probe beam positions in the horizontal plane shown in Figure 1B. The peak-to-peak signal, θ_{expt}, was measured at each probe beam position, r, obtained by careful translational adjustment of the flow cell. Along this horizontal plane, the RIG signal dropped to zero approximately at the flow cell center, and the sign on the signal changed upon probing on the opposite side of center. Both of these observations are consistent with eqs 5 and 8. Note that a collimated probe beam of dimensions much smaller than the flow cell diameter is critical for this study. In order to examine the radial dependence on the RIG sensitivity more completely, the θ_{expt} data were converted into relative angular data

$$\theta_{rel} = \frac{\theta_{expt}(r/R)}{\theta_{expt}(\max)} \qquad (12)$$

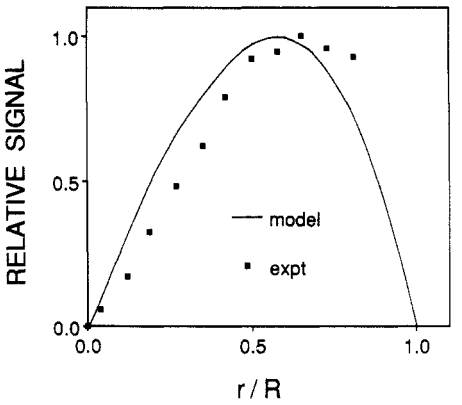

Figure 3. Relative signal, θ_{rel}, as a function of probe beam position r/R for experimentally measured RIG signals (eq 12), and the relative signal according to the Poiseuille model (eq 13). The measured RIG signals were obtained for 500 ng of dextrose (in water), injected in water at a flow rate of 50 μL/min, through a 100-cm length of 0.007 in. i.d. tubing of Teflon fluorocarbon resins coiled on a $^1/_2$ in. diameter aluminum rod.

where $\theta_{expt}(\max)$ is the maximum observed signal on the interval $0 \le r \le R$. Although both sides of the flow cell were examined ($-R \le r \le R$), due to the symmetry observed only results from $0 \le r \le R$ are shown for brevity. According to eqs 5 and 6, the model predicts θ_{rel} according to

$$\theta_{rel} = \frac{[(r/R) - (r/R)^3]}{[(1/\sqrt{3}) - (1/\sqrt{3})^3]} \qquad (13)$$

Now, θ_{rel} in both eqs 12 and 13 can be plotted as a function of r/R. The results are shown in Figure 3. Note that due to clipping of the beam at large r/R, experimental results extend only to r/R equal to 0.74. It is clear from Figure 3 that there indeed is a radial dependence on the sensitivity that is remarkably similar to that suggested by the model based upon Poiseuille flow. It was important to obtain evidence that the probe beam deflection is well behaved; i.e., deflection is along the radial axis being probed. This kind of evidence was previously unavailable due to limitations in the optical technique.

Now, since the narrow, collimated probe beam facilitated by the fiber optic-GRIN lens combination had a full beam divergence of only 3.5 mrad, it was possible to observe the deflection of the beam far-field. Photographs were taken of the probe beam as a function of time on a calibrated target at a distance of 284 cm from the flow cell. At this distance the probe beam diameter was about 1.0 cm, so a beam deflection due to a fairly concentrated analyte should be readily observed. An injection volume of 1.0 μL of 0.5% 2-propanol (by volume) was delivered to the 50 μL/min flow with the probe beam position at the optimum experimental r/R from Figure 3. Photographs were taken at 6-s intervals with the first taken 24 s after injection. The same experiment, monitored with the PSD and recorded, produced the signal shown in Figure 4. Data from the sequence of photographs taken are shown in Figure 5. The data in Figure 5 are tracings of the original photographs. Note that the beam deflection is well behaved along the radial axis being probed. The magnitude and direction of the observed signal was also correct. Slight distortion of the beam image was evident due to a small amount of clipping by the flow cell. This points toward the difficulty in aligning the flow cell. At the maximum deflection point the beam movement from baseline conditions in Figure 5 was about 0.5 cm or 1.8 mrad, consistent with the PSD measured signal in Figure 4, where the PSD was calibrated independent of this experiment. Beyond about 10 mrad for θ_{expt} the beam appeared very distorted in the far-field experiment. Below this angular deflection, the signal was well

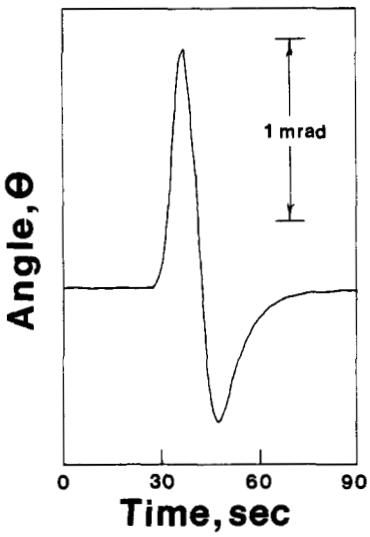

Figure 4. RIG signal recorded by the PSD from a 1-μL injected volume of a 0.5% 2-propanol solution (in water), for the same experimental conditions as in Figure 3.

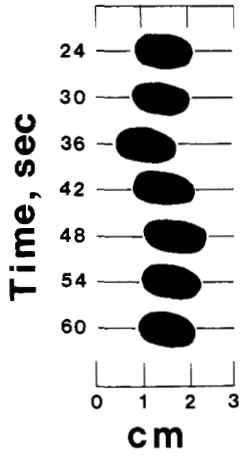

Figure 5. Tracings of photographs taken at 6-s intervals starting at 24 s for the same experimental conditions and sample as in Figure 4.

behaved and the integrated RIG response was Gaussian-like while returning to the baseline. This indicates the slight clipping of the beam was not detrimental.

The results of the experiments presented in Figures 3–5 suggest that the flow is well behaved in the flow cell leading to a sensitive means of detecting the RIG. This conclusion must be put into context with other work in the field (*11*, *25*). Peck and Morris examined the RI aberration associated with the absorbance measurement by using a commercially available wedge-shaped Z-configuration flow cell, nominally 1 mm i.d. by 1 mm path length, although R was not constant along L (*25*). Water was delivered at 2 mL/min, and the uniformity of the absorbance for an injected dye was examined by shadowgraph images. They observed a nonuniform absorbance as a function of radial position in the flow cell due to incomplete mixing. The flow pattern was not particularly ordered either (Figure 3 in ref 25). This result is not in contradiction to our results, and this can be explained in terms of the flow dynamics going into, and in, the flow cell. According to eq 14 below, an Re equal to 42 can be calculated for their experiment (*25*). The critical Reynolds number is Re equal to 2300 in a straight tube, i.e., the transition between laminar and turbulent flow (*20*), where Re is given by

$$\mathrm{Re} = \frac{2\rho F}{\pi R \eta} \tag{14}$$

where ρ is the solvent density, F the volumetric flow rate, R the tube radius, and η the solvent viscosity. The Re in the tubing leading into the flow cell was considerably higher (*25*) according to eq 14, since R (tubing) is much less than R (flow cell) and no doubt the flow is in the turbulent region, although tubing dimensions were not quoted. The wedge-shaped cell also could lead to turbulence more rapidly than a straight flow cell used in our work. The experiments, performed under conventional HPLC conditions, clearly pointed out the hydrodynamics problem associated with current absorbance detector designs (*25*). In comparison, for our work the Re is 1.1 in the flow cell and only 6.2 in the tubing leading into the flow cell for data shown in Figures 3–5. The flow is clearly in the laminar region even though flow around two rounded corners is required. The Re in the flow cell for our previous work was also in the laminar region; for example, Re was 1.3 for the separation of nanogram quantities of sugars by microbore liquid chromatography (*17*). Our experiment is consistent with the work reported by McGuffin and co-workers (*11*). They operated at Re equal to 2.1 in the flow cell and 4.3 in the entrance tubing, both in the laminar region. The radial symmetry of the RI aberration reported in their work was evident (Figure 7 in ref 11). The results shown in Figure 5 corroborate with this report (*11*), but our focus is to further demonstrate how a RI problem can be turned into a sensitive RIG detector.

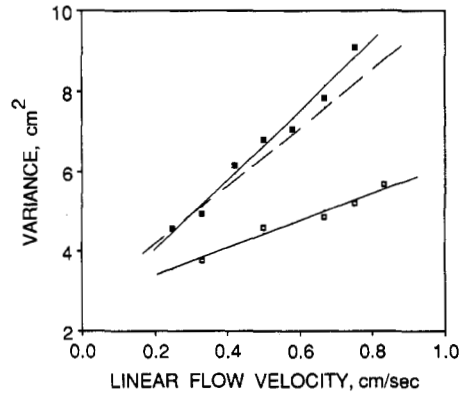

Figure 6. Toluene peak variance data (σ_x^2) in the context of the RIG detector flow cell, as a function of the linear flow velocity in the flow cell: (□) variance data obtained by using the absorbance detector and best fit line (eq 15); (■) variance data obtained by using the RIG detector and best fit line (eq 16). The dashed line is the sum of the absorbance detector line (*15*) and the predicted variance contribution due to the RIG detector flow cell (eqs 3 and 17). As a reference point, note that before converting the data to length variances, that the base width volume of the toluene peak at 0.33 cm/s (100 μL/min) was 45 μL, while the flow cell volume was 5.0 μL.

Attention was then turned to examining the credibility of eq 11 for predicting the angular sensitivity of the RIG measurement. A critical evaluation of band broadening as a function of the linear flow velocity (eq 9) was required. Toluene, serving as a test analyte, was chromatographically retained and detected by using a commercially available absorbance detector and also the RIG detector. The detectors were employed in successive experiments. The absorbance detector employed a small-volume flow cell that introduced negligible band broadening compared to the RIG detector, thus providing, to a good approximation, a measure of the chromatographic broadening, σ_v. Likewise, the band broadening observed for the RIG detector was also measured. Both sets of band-broadening data were converted into length variance data, σ_x^2, in the context of the RIG detector flow cell (*24*). The results are shown in Figure 6, where σ_x^2 is plotted as a function of the linear flow velocity, u, in the flow cell. Both detectors fit a linear function. For the absorbance detector

$$\sigma_x^2 = 3.48u + 2.67 \tag{15}$$

and for the RIG detector

$$\sigma_x^2 = 8.74u + 2.27 \quad (16)$$

The solid lines in Figure 6 correspond to eqs 15 and 16. Within experimental uncertainty the y intercepts are essentially equal, corresponding to the chromatographic band-broadening A-term (26). With both detectors, the resulting band broadening also exhibits a term that is linearly related to u, i.e., the C-term (26). The difference between the data obtained with the two detectors is primarily in the term proportional to u. For this set of experiments with the RIG detector, the flow cell diameter was 0.80 mm. The Re was 10 at the highest flow rate for this flow cell, thus within the laminar range. The RIG detector contributes to the band broadening according to eq 3, as described in the context of the chromatographic broadening in eq 9. The predicted band broadening for the RIG detector is described by the following equation:

$$\sigma_x^2 = 3.89u \quad (17)$$

Since the dimensions of the absorbance detection flow cell were chosen to not introduce significant band broadening, it is reasonable to expect that the sum of eqs 15 (chromatographic variance) and 17 (RIG detector variance) should predict the measured variance for the RIG detector. The sum of eqs 15 and 17 is given by

$$\sigma_x^2 = 7.37u + 2.67 \quad (18)$$

Equation 18 is shown as a dashed line in Figure 6. Reasonable agreement between eqs 16 and 18 was obtained. Although the additional band broadening due to the RIG detector flow cell seems somewhat large for routine LC application, note that the experiment was purposely designed to examine the σ_x^2 and u dependencies. In addition to the hydrodynamic band broadening in the flow cell described by eq 3, in the context of the flow cell and chromatographic peak variance (eq 9), the RIG signal will be reduced slightly due to a "number-averaging effect" since the signal is actually averaged over the probe beam path length. For the toluene data, with approximately a 50 μL wide peak at the base and the 5 μL volume flow cell, the number-averaging effect accounted for less than a 2% decrease in sensitivity. Thus, the number-averaging effect was considered negligible for this work.

The credibility of eq 11 was examined by comparing the relative RIG signal, θ_{rel}, from experimentally measured angle data to θ_{rel} predicted from the σ_x^2 and u (flow cell) dependencies. A comparison of θ_{rel} over a range of flow rates is made instead of comparing absolute θ in order to minimize the bias associated with small uncertainties in the other parameters in eq 11. According to eqs 11 and 18, θ_{pred} should be related by

$$\theta_{pred} \propto \frac{u}{7.37u + 2.67} \quad (19)$$

The maximum in θ_{expt} occurred at u equal to 0.67 cm/s, i.e., 200 μL/min (in the flow cell), so θ_{rel} from measured angular data was defined as

$$\theta_{rel} = \frac{\theta_{expt}(u)}{\theta_{expt}(0.67)} \quad (20)$$

In order to properly compare eq 20 to the predicted θ_{rel}, u equal to 0.67 must also be used as the reference point. The predicted θ_{rel} follows from eq 19 and is given by

$$\theta_{rel} = \frac{u}{0.65u + 0.24} \quad (21)$$

Equations 20 and 21 are shown in Figure 7. For the lower flow rates, there is excellent agreement between the two approaches for obtaining θ_{rel}, suggesting that the model does predict the relative sensitivity of the RIG detector at low Re. Beyond 200 μL/min the sensitivity of the RIG response fell off from that predicted by eq 22, possibly indicating a change in hydrodynamics in the flow cell. Figures 6 and 7 indicate that even though the RIG detector introduces some band broadening, the sensitivity actually increases due to the dependence of u in the numerator of eq 11 (and eq 21).

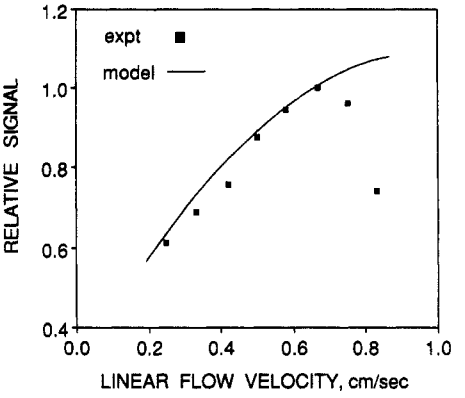

Figure 7. Comparison of the experimentally measured relative angle and the predicted relative angle, as a function of linear flow velocity. The toluene peak variance data presented in Figure 6 and the experimentally obtained RIG signals were applied in eqs 21 and 20, respectively, for the comparison.

Table I. Experimental Values of Parameters Used in Predicting θ by Applying Equation 11

V_i	injected volume	4×10^{-3} cm^3
C_i	injected volume fraction	1.36×10^{-4}
u	linear flow velocity in flow cell	0.33 cm/s
σ_x^2	length variance in flow cell	5.1 cm^2 (eq 18)
D_m	analyte diffusion coefficient	1.7×10^{-5} cm^2/s (estimated from ref 27)
R	flow cell radius	0.04 cm
L	path length orthogonal to probed concentration gradient	1.0 cm
n_o	solvent RI	1.34
dn/dC	toluene in 50% water/50% acetonitrile	0.14 (calculated from ref 28)

The utility of eq 11 to predict the absolute measured angle θ_{expt} from known experimental parameters was examined. A sample calculation was performed for toluene as the test analyte. At a flow rate of 100 μL/min, the band-broadening contribution due to the RIG detector was only about 16%, thus eq 11 will be accurately followed. The salient experimental parameters are listed in Table I. θ_{expt}, measured at the optimum r/R position was 120 μrad. θ_{pred} calculated from eq 11 by using the values in Table I was 160 μrad. Note in the calculation that the constant in eq 11 is 2 times 0.0146 for the peak-to-peak signal. There is excellent agreement between these two figures, indicating, in conjunction with Figure 7, that the model reasonably predicts the observed sensitivity of this RIG detector at low Re. Although band broadening was purposely introduced in this work to elucidate the detection mechanism, one could minimize the flow cell contribution to band broadening by using a smaller R and L. According to eqs 3, 9, and 11, both of these design changes will decrease the flow cell contribution to band broadening, but the price is decreased detection sensitivity as well. A compromise between minimizing broadening and maximizing detection sensitivity results.

It is instructive to consider the design of a flow cell that would be suitable for microbore liquid chromatography, i.e., by not introducing significant band broadening, while maintaining useful detection sensitivity and functioning at typical

microbore liquid chromatography flow rates. A useful flow cell design for microbore liquid chromatography would have a 400-μm radius and a 5-mm length, producing a 2.5-μL volume. At a typical flow rate of 25 μL/min and an analyte D_m of 2×10^{-5} cm^2/s, eq 3 predicts a length variance contribution of 0.14 cm^2 due to the flow cell. The Reynolds number would be 0.67 for a mobile phase like water, thus consistent with this work and clearly in the Poiseuille flow region. The analyte peak will have a base width volume of 25 μL by using a 25 cm length by 1 mm i.d. microbore column that produces 24 000 plates/m and assuming an analyte capacity factor k equal to 3 and a typical dead volume of 120 μL; i.e., a maximum of 10% of the peak will be in the flow cell at any instant. Under these conditions the hydrodynamic band-broadening effect due to the flow cell, described by eq 9, will reduce the RIG signal by only 8.9%. Similarly, the number-averaging effect due to the integration of the RIG over the flow cell path length reduces the signal by only 1.3%. Thus, under useful microbore efficiency conditions, the described flow cell will introduce about a 10% decrease in sensitivity from the "ideal". When the analyte peak volume is doubled to 50 μL, i.e., at 6000 plates/m, the total band broadening introduced decreases the sensitivity by less than 3%. Clearly, a flow cell can be designed that is useful for microbore liquid chromatography. Indeed, we have recently constructed a flow cell for microbore liquid chromatography and applied the RIG detector with both conventional mobile-phase gradient and thermal gradient microbore liquid chromatography (*29*).

For these microbore liquid chromatography conditions, a sensitivity comparison between probing the radial concentration $dC(r)/dr$ reported here and the axial concentration gradient $dC(o)/dx$ (*18*, *19*) follows from eq 6. For an analyte with D_m equal to 2×10^{-5} cm^2/s (small molecule), at 25 μL/min (0.083 cm/s), and with a flow cell radius of 0.04 cm at constant path length, one obtains

$$dC(r)/dr = 32(dC(o)/dx) \qquad (22)$$

indicating a substantial gain in sensitivity in RIG detection by probing the radial concentration gradient over the axial concentration gradient. It was impractical to measure $dC(o)/dx$ directly with our apparatus in order to examine eq 22 experimentally, but the evidence presented indicates that $dC(r)/dr$ can be successfully measured. Additionally, eq 10 suggests that there is a path length advantage in probing $dC(r)/dr$ instead of $dC(o)/dx$. For the 0.5 cm length by 0.08 mm diameter flow cell, the path length advantage is 6.3. Combining this result with the concentration gradient ratio (eq 23) yields an overall sensitivity improvement factor of over 200. Note also that as the analyte D_m decreases from that of a small molecule, such as for a macromolecule, eq 6 predicts an improvement in sensitivity.

The obvious application for this detector is microbore liquid chromatography (*15*, *17*, *29*). In the proper Reynolds number range, a suitable flow cell for conventional liquid chromatography could also be readily constructed. In the future, the potential for employing radial-diffusion-controlled RIG detection with separation methods based upon laminar flow seems ideal, such as in field flow fractionation (*30*). The detection model should also be useful in interpreting molecular weight dependencies and subsequent availability of useful information in the HPLC application of this RIG detector. It will also be important to translate the enhanced sensitivity into enhanced detectability by critically examining and utilizing methods to reduce the noise in the measurements (*31*).

LITERATURE CITED

(1) Taylor, G. *Proc. R. Soc. (London)* **1953**, *A219*, 186–203.
(2) Vanderslice, J. T.; Stewart, K. K.; Rosenfeld, A. G.; Higgs, D. J. *Talanta* **1981**, *28*, 11–18.
(3) Vanderslice, J. T.; Rosenfeld, A. G.; Beecher, G. R. *Anal. Chim. Acta* **1986**, *179*, 119–129.
(4) Ruzicka, J.; Hansen, E. H. *Anal. Chim. Acta* **1978**, *99*, 37–76.
(5) Tijssen, R. *Anal. Chim. Acta* **1980**, *114*, 71–89.
(6) Deelder, R. S.; Kroll, M. G. F.; Beeren, A. J. B.; Van Den Berg, J. H. M. *J. Chromatogr.* **1978**, *149*, 669–682.
(7) Golay, M. J. E.; Atwood, J. G. *J. Chromatogr.* **1979**, *186*, 353–370.
(8) Atwood, J. G.; Golay, M. J. E. *J. Chromatogr.* **1981**, *218*, 97–122.
(9) Katz, E. D.; Scott, R. P. W. *J. Chromatogr.* **1983**, *270*, 29–50.
(10) Grushka, E.; Kikta, E. J., Jr. *J. Am. Chem. Soc.* **1976**, *98*, 643–648.
(11) Evans, C. E.; Shabushnig, J. G.; McGuffin, V. L. *J. Chromatogr.* **1988**, *459*, 119–138.
(12) Renn, C. N.; Synovec, R. E. *Anal. Chem.* **1990**, *62*, 558–564.
(13) Renn, C. N.; Synovec, R. E. *Anal. Chem.* **1988**, *60*, 1188–1193.
(14) Renn, C. N.; Synovec, R. E. *Appl. Spectrosc.* **1989**, *43*, 1393–1398.
(15) Hancock, D. O.; Synovec, R. E. *Anal. Chem.* **1988**, *60*, 1915–1920.
(16) Hancock, D. O.; Synovec, R. E. *Anal. Chem.* **1988**, *60*, 2812–2818.
(17) Hancock, D. O.; Synovec, R. E. *J. Chromatogr.* **1989**, *464*, 83–91.
(18) Pawliszyn, J. *Anal. Chem.* **1986**, *58*, 243–246.
(19) Pawliszyn, J. *Anal. Chem.* **1986**, *58*, 3207–3215.
(20) Kachel, V.; Menke, E. In *Flow Cytometry and Sorting*; Melamed, M. R., Mullaney, P. F., Mendelsohn, M. L., Eds.; John Wiley: New York, 1979; Chapter 3, pp 41–59.
(21) Whitaker, S. *Introduction to Fluid Mechanics*; Prentice-Hall: Englewood Cliffs, NJ, 1968; Chapter 7, pp 235–247.
(22) West, R. C., Ed. *CRC Handbook of Chemistry and Physics*, 67th ed.; CRC Press: Boca Raton, FL; 1986; p F-96.
(23) Hupe, K.-P.; Jonker, R. J.; Rozing, G. *J. Chromatogr.* **1984**, *285*, 253–265.
(24) Giddings, J. C. *Dynamics of Chromatography*; Marcel Dekker: New York, NY, 1965; Chapter 2, p 83.
(25) Peck, K.; Morris, M. D. *J. Chromatogr.* **1988**, *448*, 193–201.
(26) Karger, B. L.; Snyder, L. R.; Horvath, C. *An Introduction to Separation Science*; Wiley-Interscience: New York, NY, 1973; Chapter 5, pp 144–145.
(27) Gruska, E.; Kitka, E. J., Jr. *J. Phys. Chem.* **1974**, *78*, 2297–2301.
(28) Synovec, R. E.; Yeung, E. S. *Anal. Chem.* **1983**, *55*, 1599–1603.
(29) Synovec, R. E.; Renn, C. N. Presented at the 14th International Symposium on Column Liquid Chromatography, Boston, MA, May 22, 1990.
(30) Giddings, J. C.; Yang, F. J.; Myers, M. N. *Anal. Chem.* **1976**, *48*, 1126–1132.
(31) Bialkowski, S. E.; He, Z. F. *Anal. Chem.* **1988**, *60*, 2674–2679.

RECEIVED for review May 7, 1990. Accepted August 6, 1990. We thank the National Science Foundation Center for Process Analytical Chemistry for partial support of this work.